Turkish Journal of Electrical Engineering & Computer Sciences

http://journals.tubitak.gov.tr/elektrik/

Research Article

Turk J Elec Eng & Comp Sci
(2016) 24: 1075 – 1090

doi:10.3906/elk-1312-108

Artificial bee colony algorithm based optimal reactive power flow of two-terminal HVDC systems

Ulaş KILIÇ[1,*], **Kürşat AYAN**[2]

[1]Department of Mechatronics Engineering, Faculty of Hasan Ferdi Turgutlu Technology, Celal Bayar University, Turgutlu, Manisa, Turkey

[2]Department of Computer Engineering, Faculty of Computer and Information Science, Sakarya University, Adapazarı, Sakarya, Turkey

Received: 14.12.2013 • **Accepted/Published Online:** 08.02.2014 • **Final Version:** 23.03.2016

Abstract: This paper presents a solution technique for the optimal reactive power flow (ORPF) of alternating current-direct current (AC-DC) power systems using the artificial bee colony (ABC) algorithm. A high voltage direct current (HVDC) transmission link is one of the most important network components in AC-DC power systems. In recent years there has been an increasing number of studies related to power systems with HVDC transmission links. One of them is the reactive power flow (RPF) optimization. The aim of ORPF in alternating current (AC) or AC-DC power systems is to minimize transmission line power loss under equality and inequality constraints. The relationships related to the HVDC link are incorporated into AC power system equations considering its power transfer characteristics. This paper contributes to the solution of the problem by using the ABC algorithm for the first time. The proposed method is examined on three test systems and its effectiveness in these kinds of applications is shown by the comparative results.

Key words: Optimal reactive power flow, HVDC system, ABC algorithm

1. Introduction

Scientists have been trying to solve the ORPF problem in power systems for a long time [1–5]. The aim of ORPF in alternating current (AC) or AC-DC power systems is to minimize an objective function, which is the power loss of the transmission lines under equality and inequality constraints. The power equalities for entire buses in an AC power system are considered as the equality constraints. The physical constraints related to the power system are considered as the inequality constraints. All constraints of the problem must be satisfied while the power loss is being minimized.

A lot of methods (numerical and heuristic) have been used for solving the ORPF problem of AC power systems so far [1–13]. It can be said that the heuristic methods have many advantages in comparison with numerical methods from the results reported in the literature [4–13]. For examples, heuristic methods converge faster than the others, the convergence of the algorithm is independent of the initial conditions of the optimization, and the algorithm is not caught in a local minimum.

The generation and transmission capacity of power systems must be increased as energy consumption has been increasing in recent years. Due to this increase in energy consumption, transmission lines can be overloaded and some generators in the network can be out of synchronism even when the network is subjected to minor

*Correspondence: ulas.kilic@cbu.edu.tr

disturbances. In order to maintain continuity of operating, the network must be rescheduled by the power system planners. Recently HVDC links have been used extensively for power transmission within a network. The power transmission using HVDC links has many advantages. One of them is that only active power is transferred through HVDC links. The other one is that the instantaneous power in an AC power system can be controlled by means of HVDC links. Furthermore, stabilization of the power systems can be satisfied by using HVDC links [14]. A lot of research on OPF and ORPF of integrated AC-DC power systems has been conducted recently [15–19]. The dynamics of two-terminal HVDC links have also been proposed [20].

For solution of the ORPF problem of AC-DC systems, DC link dynamics are included in the problem. Two basic approaches were developed for performing the power flow so far. The first one is the sequential approach [19,21–22] and the second is the unified approach [23]. In the first approach the solution of AC and DC system equations is performed sequentially. Even though the application of the sequential method is simple, it converges to the local minimum for certain conditions. In this approach DC variables are not part of the state vector. In the current study the first approach is preferred.

The OPF and ORPF problems of power systems are nonlinear and nonconvex mathematical problems. Various population-based heuristic optimization algorithms have been developed for the solution of this kind of problem in recent years. One of them is the ABC algorithm proposed by Derviş Karaboğa [24]. Because this is an effective algorithm for determining the global minima of this kind of problems, it could be applied successfully to the power system problems [25–29]. In the current study the ABC algorithm is used for the solution of the ORPF problem of two-terminal HVDC systems for the first time.

In this study the transformers are represented by their real models. In the real transformer model the tap ratios of the transformers change to their impedances. As a result of this, the bus admittance matrix of the power system must be modified continuously during the power flow analysis. For this reason they are selected as the control variables. Thus, the power flow calculations can be implemented without including the impact of the transformers in the Jacobian matrix. In the ABC algorithm, because each individual selects a distinct tap ratio for each transformer and the bus admittance matrix of the system is calculated uniquely for each one, this process increases the computational time of the software.

The modeling of the DC transmission link is represented in section 2. Per unit system relationships are given in section 3. The methodology of the ABC algorithm is explained in section 4. ABC algorithm-based ORPF solution of HVDC systems is illustrated in section 5. To show its effectiveness, comparative simulation results of three test systems having a two-terminal HVDC link are provided in section 6. The conclusions are discussed in section 7.

2. Modeling of the DC transmission link

Modeling of the DC link and the converter is needed for the analysis of HVDC power systems. This process is based on the accepted assumptions in [23].

A general bus representation having generators, AC lines, shunt reactive compensators, and converters is given in Figure 1 [30].

In Figure 1, P, Q, V, and δ represent active power, reactive powers, bus voltage magnitudes, and angles, respectively. The subscripts g, l, s, and d represent generator, load, shunt reactive compensator, and DC link, respectively. The active and reactive power balances for such a bus are formulated by Eqs. (1) and (2).

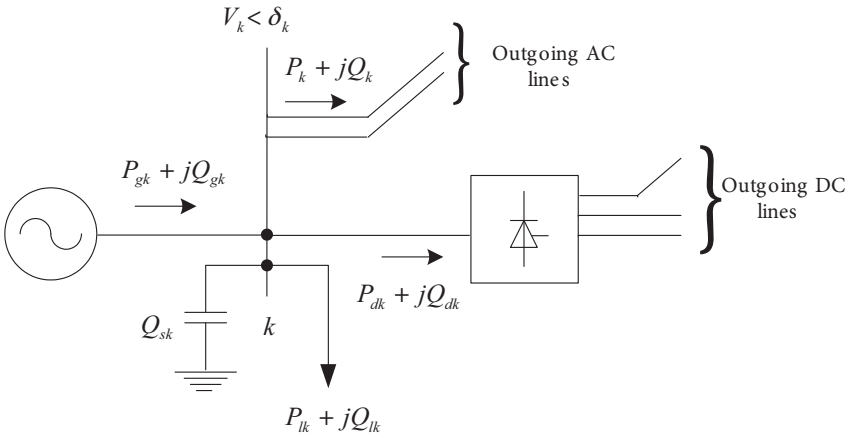

Figure 1. The AC bus representation with DC link [30].

$$P_{gk} = P_{lk} + P_{dk} + P_k \tag{1}$$

$$Q_{gk} + Q_{sk} = Q_{lk} + Q_{dk} + Q_k, \tag{2}$$

where P_{gk} and Q_{gk} represent the output active and reactive powers of the generator connected to the k^{th} bus, P_{lk} and Q_{lk} represent the active and reactive loads of the k^{th} bus, Q_{sk} represents the reactive power of the shunt compensator connected to the k^{th} bus, P_{dk} represents the active power given to the dc transmission link connected to the k^{th} bus, Q_{dk} represents the reactive power absorbed by the converter at the k^{th} bus, P_k and Q_k represent the active and reactive powers transferred through the AC transmission line connected to the k^{th} bus. P_k and Q_k are also given by the following equations:

$$P_k = V_k \sum_{j=1}^{N} V_j \left(G_{kj} \cos \delta_{kj} + B_{kj} \sin \delta_{kj}\right) \tag{3}$$

$$Q_k = V_k \sum_{j=1}^{N} V_j \left(G_{kj} \sin \delta_{kj} - B_{kj} \cos \delta_{kj}\right), \tag{4}$$

where V_j and V_k are the voltage magnitudes of the j^{th} and k^{th} buses; G_{kj} and B_{kj} are the transfer conductance and susceptance between buses k and j of the bus admittance matrix Y_{bus}; δ_{kj} is the voltage angle difference between buses k and j; N is the bus number in the power system.

The power relationships for the rectifier bus can be given by the following equations:

$$P_{dk} = P_{dr} \tag{5}$$

$$Q_{dk} = Q_{dr} \tag{6}$$

The power relationships for the inverter bus can be given by the following equations:

$$P_{dk} = -P_{di} \tag{7}$$

$$Q_{dk} = Q_{di}, \tag{8}$$

where P_{dr} and P_{di} represent active powers at rectifier and inverter terminals, respectively. Q_{dr} and Q_{di} represent reactive powers absorbed by the rectifier and inverter terminals, respectively.

A representation of a two-terminal HVDC link between rectifier (r) and inverter (i) buses is given in Figure 2. The converter formulations describing the relationship between AC and DC variables are illustrated in [31].

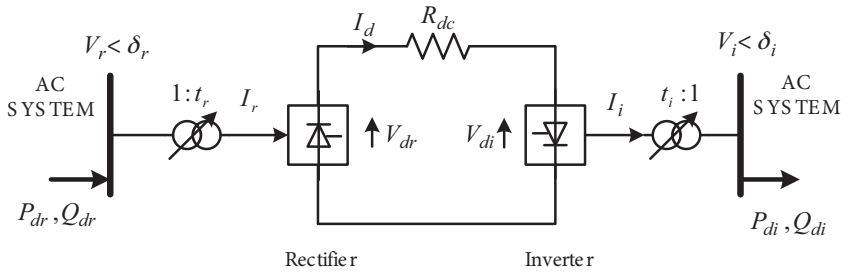

Figure 2. A representation of a two-terminal HVDC link [31].

In Figure 2, I_r and I_i are AC currents at rectifier and inverter terminals, V_{dr} and V_{di} are DC voltages at rectifier and inverter terminals, I_d is the DC current, t is the effective transformer tap ratio.

An equivalent circuit of a two-terminal HVDC link is shown in Figure 3 [32]. The voltage relationships for rectifier operation can be given by the following equations:

$$V_{dor} = \frac{3\sqrt{2}}{\pi} V_r t_r \tag{9}$$

$$V_{dr} = V_{dor} \cos\alpha - R_{cr} I_d, \tag{10}$$

where V_{dor} and V_{dr} are DC voltages at rectifier terminal for unload (open circuit) and loaded cases, and α is the excitation angle for the rectifier. R_{cr} is named equivalent commutating resistance, which accounts for the voltage drop due to commutation overlap. It is proportional to the commutation reactance X_{cr} and is represented by $R_{cr} = 3X_{cr}/\pi$. The active power at the rectifier terminal is determined by the following equation:

$$P_{dr} = V_{dr} I_d \tag{11}$$

The losses of the converter and transformer can be neglected ($P_{dr} = P_{ac}$) and so the reactive power absorbed by the rectifier can be given by the following equation:

$$Q_{dr} = \left| P_{dr} \tan\varphi_r \right|, \tag{12}$$

where φ_r is the phase angle between the AC voltage and the fundamental component of the AC current at the rectifier terminal and is calculated by ignoring the commutation overlap by the following equation:

$$\varphi_r = \cos^{-1}\left(V_{dr}/V_{dor}\right) \tag{13}$$

The whole relationships for the inverter operation can be given by the following equations:

$$V_{doi} = \frac{3\sqrt{2}}{\pi} V_i t_i \tag{14}$$

$$V_{di} = V_{doi}\cos\gamma - R_{ci}I_d \tag{15}$$

$$P_{di} = V_{di}I_d \tag{16}$$

$$Q_{di} = |P_{di}\tan\varphi_i| \tag{17}$$

$$\varphi_i = \cos^{-1}\left(V_{di}/V_{doi}\right), \tag{18}$$

where V_{doi} and V_{di} are DC voltages at the inverter terminal for unload (open circuit) and loaded cases, γ is the extinction angle for the inverter, and R_{ci} is named equivalent commutating resistance of the inverter terminal and is represented by $R_{ci} = 3X_{ci}/\pi$; φ_i is the phase angle between the AC voltage and the fundamental component of the AC current at the inverter terminal.

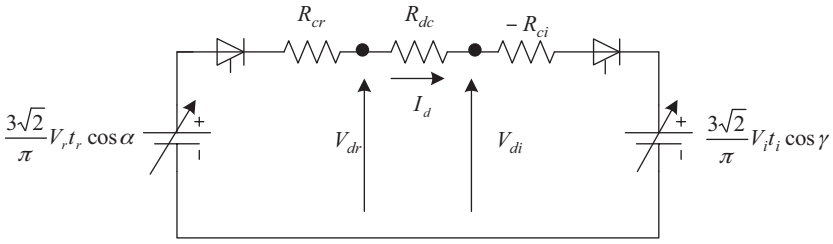

Figure 3. The equivalent circuit of a two-terminal HVDC link [32].

By defining R_{dc} DC link resistance, the relationship between the voltages at the rectifier and inverter terminals of the DC link can be given by the following equation:

$$V_{dr} = V_{di} + R_{dc}I_d \tag{19}$$

3. Per unit system equations

Actual system equations and per unit system equations are represented by capital and small letters, respectively. The base quantities P_{base} and V_{acbase} are firstly determined and then the base quantities I_{acbase} and Z_{acbase} can be given with reference to these quantities by the following relationships:

$$P_{acbase} = P_{base} \tag{20}$$

$$I_{acbase} = \frac{P_{acbase}}{\sqrt{3}V_{acbase}} \tag{21}$$

$$Z_{acbase} = \frac{V_{acbase}}{\sqrt{3}I_{acbase}} \tag{22}$$

In terms of the base quantities defined above, whole per unit system relationships can be given by the following equations:

$$v = \frac{V}{V_{acbase}} \tag{23}$$

$$v_d = \frac{V_d}{V_{acbase}} \tag{24}$$

$$i_d = \frac{I_d}{I_{acbase}} \tag{25}$$

$$x_c = \frac{X_c}{Z_{acbase}} \tag{26}$$

$$p_d = \frac{P_d}{P_{acbase}} \tag{27}$$

The actual DC link voltage is calculated by the following equation:

$$V_d = Vnkt\frac{\sqrt{2}}{\pi}\sin\left(\frac{\pi}{k}\right)\cos\alpha - \frac{nkX_c}{2\pi}I_d, \tag{28}$$

where n is the bridge number in series and k is the peak number on the load per period. For $k = 6,\ n = 1$:

$$V_d = \frac{3\sqrt{2}}{\pi}Vt\cos\alpha - \frac{3X_c}{\pi}I_d \tag{29}$$

dividing Eq. (29) by V_{acbase}

$$\frac{V_d}{V_{acbase}} = \frac{\frac{3\sqrt{2}}{\pi}Vt\cos\alpha}{V_{acbase}} - \frac{\frac{3X_c}{\pi}I_d}{V_{acbase}} \tag{30}$$

$$\frac{V_d}{V_{acbase}} = \frac{\frac{3\sqrt{2}}{\pi}Vt\cos\alpha}{V_{acbase}} - \frac{\frac{3X_c}{\pi}I_d}{\sqrt{3}Z_{acbase}I_{acbase}} \tag{31}$$

Per unit DC system equations are calculated by the following relationships:

$$v_d = \frac{3\sqrt{2}}{\pi}vt\cos\alpha - \frac{\sqrt{3}}{\pi}x_c i_d \tag{32}$$

$$p_d = v_d i_d \tag{33}$$

The DC voltage for an unload (open circuit) case is expressed by the following equation:

$$v_{do} = \frac{3\sqrt{2}}{\pi}vt \tag{34}$$

The phase angle between the AC voltage and the fundamental component of the AC current is given by the following equation:

$$\varphi = \cos^{-1}\left(v_d/v_{do}\right) \tag{35}$$

The reactive power absorbed by the converters is given by the following equation:

$$q_d = |p_d\tan\varphi_d| \tag{36}$$

4. Overview of the ABC algorithm

The artificial bee colony algorithm (ABC) was proposed by Derviş Karaboğa in 2005 by using the swarm intelligence of real bees. This algorithm has been applied to and used for the successful solution of various engineering problems since the time it was proposed [33–35]. The ABC algorithm consists of four major steps: initialization, worker bees, onlooker bees, and scout bees. Following the initialization step, the other three steps are repeated respectively until the algorithm is completed.

The following assumptions shall be noted before getting into the other steps: only one bee can enter into each source of nourishment; a *failure* value is saved for each source of nourishment; the bees that are sent to the nourishment sources at the initialization step are considered as worker bees after this step.

Initialization: at this step nourishment sources within the search area are randomly identified. In order to identify a nourishment source, a random value between the lower limit and the upper limit of the parameters can be deduced by using the equation below:

$$w_{ij}^{new} = w_{\min,j} + rand(0,1) \times (w_{\max,j} - w_{\min,j}) \quad i = 1, ..., SN \quad j = 1, ..., D, \tag{37}$$

where SN is the size of the nourishment source, D is the number of optimization parameters, $w_{\min,j}$ and $w_{\max,j}$ are the limits of the nourishment source position, and $rand(0,1)$ varies between 0 and 1.

Step 1. Worker bees: the worker bees identify a new nourishment source neighboring the nourishment source they work on; if the amount of nectar in the given source is abundant, the newly detected source gets memorized. The worker bee then informs the other bees in the hive which sources are the best. The identification process of the new nourishment sources can be defined below:

$$w_{ij}^{new} = w_{ij}^{old} + \lambda_{ij} \left(w_{ij}^{old} - w_{kj}^{old} \right) \quad i = 1, ..., SN \quad k = 1, ...,SN \quad j = 1, 2, ...,D \quad i \neq k, \tag{38}$$

where w_{ij} is the nourishment source position, and λ_{ij} is a random number between –1 and 1.

Step 2. Onlooker bees: each one of the worker bees informs the scout bees about the nourishment source they have used. The scout bees then designate a nourishment source in proportion with the amount of nectar in the source. The designation probability of a particular nourishment source is determined by the ratio of the amount of nectar in this nourishment source to the total amount of nectar in all sources. This ratio is determined by Eq. (39). This operation is called the roulette wheel [36]. In this way the nourishment sources with larger amounts of nectar have higher designation chances.

$$sp_i = \frac{fit_i}{\sum_{j=1}^{SN} fit_j}, \tag{39}$$

where fit_i represents the amount of nectar of the i^{th} nourishment source, which is its proportional to the fitness value.

The efficiency of a nourishment source is calculated by Eq. (40) [33–35]. The designation probability of nourishment sources having a high efficiency is higher in roulette wheel selection.

$$fit_i = \frac{1}{F_i} \tag{40}$$

Step 3. Scout bees: at the end of each cycle when all worker bees and scout bees finish their quest for sources, they share the information they have collected with the other bees in the beehive. This sharing of information also includes the failure value of each nourishment source. This measurement technique shows whether the nourishment source with the largest amount of nectar in a given region is depleted or not. If the source with the larger amount of nectar is depleted, the search for nourishment around that source discontinues. In that case, the worker bee leaves that given nourishment source and the scout bees discontinue their search around that source. If a worker bee leaves a particular source, then that very bee becomes a scout bee. In each cycle only one bee among all worker bees can become a scout bee. When a worker bee becomes a scout bee, then the

new scout bee randomly identifies a new nourishment source in the search area using Eq. (37). The equation value to determine that a particular source is depleted is referred to as the "limit". The flowchart of the ABC algorithm is given in Figure 4.

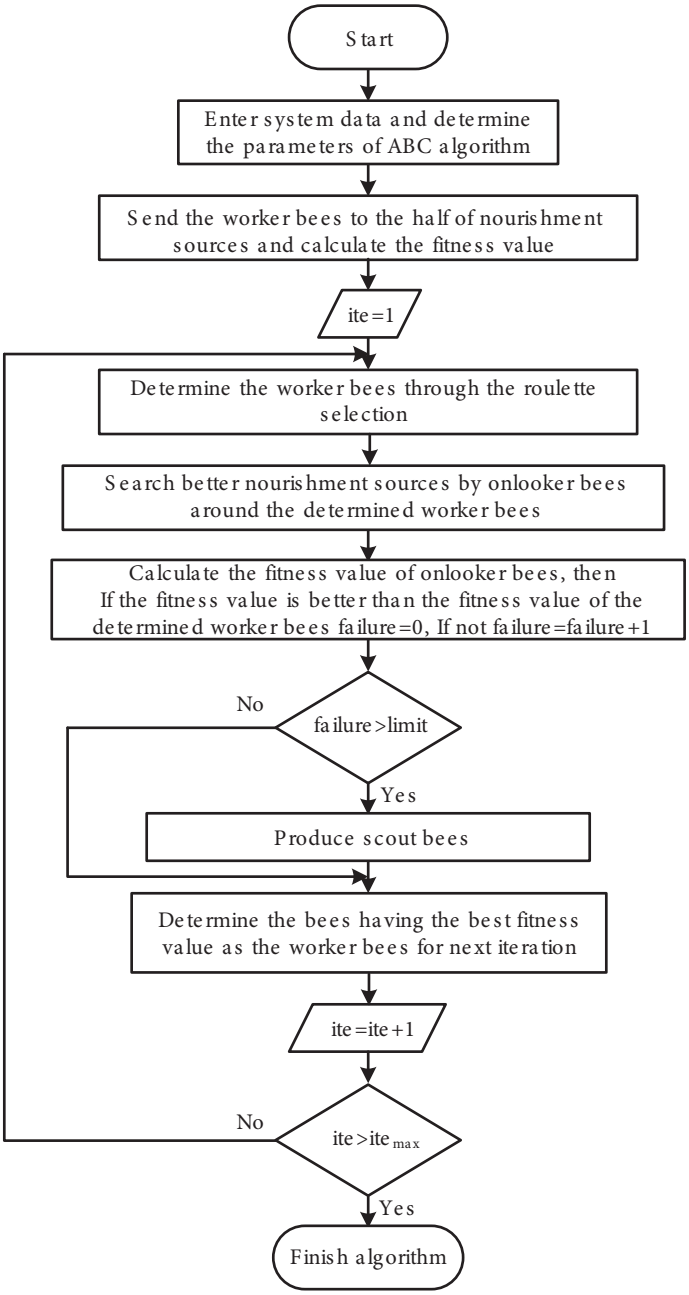

Figure 4. Flowchart of the ABC algorithm.

5. Application of the ABC algorithm to ORPF of HVDC systems

The control and state variables of an AC-DC system should be determined by considering the nature of the problem. These variables are chosen as follows:

$$u = [u_{AC},\, u_{DC}] \tag{41}$$

$$u_{AC} = [p_{g2}, ..., p_{gNg}, v_{g1}, ..., v_{gNg},\, q_{s1}, ..., q_{sN_s},\, t_1, ..., t_{N_T}] \tag{42}$$

$$u_{DC} = [p_{dr},\, p_{di},\, q_{dr},\, q_{di}, i_d]\,, \tag{43}$$

where p_{gi} is the generator active power outputs (except for the slack bus), v_{gi} is the generator voltages, N_g is the number of generator buses, N_s is the number of shunt compensators, and N_T is the number of transformers.

The state variables are also determined as follows:

$$x = [x_{AC},\, x_{DC}] \tag{44}$$

$$x_{AC} = [p_{gslack},\, q_{g1}, ..., q_{gNg},\, v_{l1}, ..., v_{lN_l}] \tag{45}$$

$$x_{DC} = [t_r,\, t_i,\, \alpha,\, \gamma, v_{dr}, v_{di}]\,, \tag{46}$$

where p_{gslack} is the slack bus active power output, q_{gi} is the reactive power outputs, v_{li} is the load bus voltages, and N_l is the number of load buses.

We update the active and reactive power at rectifier and inverter terminals by the following equations:

$$\begin{array}{l} p_{load}^{update} = p_{load} + p_{dr} \\ q_{load}^{update} = q_{load} + q_{dr} \end{array} \tag{47}$$

$$\begin{array}{l} p_{load}^{update} = p_{load} - p_{di} \\ q_{load}^{update} = q_{load} + q_{di} \end{array} \tag{48}$$

A fitness value F_i for each bee is calculated by the following equation:

$$\begin{array}{l} F_i = K_1 p_{Loss} + K_2 \left| p_{gslack} - p_{gslack}^{\lim} \right| + K_3 \sum\limits_{i=1}^{N_g} \left| q_{gi} - q_{gi}^{\lim} \right| + K_4 \sum\limits_{i=1}^{N_l} \left| v_{li} - v_{li}^{\lim} \right| \\ + K_5 \left| t_r - t_r^{\lim} \right| + K_6 \left| t_i - t_i^{\lim} \right| + K_7 \left| \alpha - \alpha^{\lim} \right| + K_8 \left| \gamma - \gamma^{\lim} \right| + K_9 \left| v_{dr} - v_{dr}^{\lim} \right| + K_{10} \left| v_{di} - v_{di}^{\lim} \right| \end{array}, \tag{49}$$

where $p_{gslack}^{\lim}$, $q_{gi}^{\lim}$, $v_{li}^{\lim}$, $t_r^{\lim}$, $t_i^{\lim}$, $\alpha^{\lim}$, $\gamma^{\lim}$, $v_{dr}^{\lim}$, and $v_{di}^{\lim}$ represent the limits of the corresponding variables, and the constants of K are the penalty weights of the corresponding variables.

A fitness value F_i is calculated for each bee step by step as follows:

Step 1: Update p_{load} and q_{load} at converter terminals by Eqs. (47) and (48)

Step 2: Run Newton–Raphson power flow software

Step 3: The phase angle at converter terminals is calculated by Eq. (50):

$$\varphi = \arctan\left(\frac{q_d}{p_d}\right) \tag{50}$$

Step 4: The loaded DC voltage at converter terminals is calculated by Eq. (51):

$$v_d = \frac{p_d}{i_d} \tag{51}$$

Step 5: Calculate the unload DC voltage at rectifier and inverter terminals by Eq. (52):

$$v_{do} = \frac{v_d}{\cos\varphi} \tag{52}$$

Step 6: Calculate the tap ratio at each converter terminal by Eq. (53):

$$t = \frac{v_{do}}{\frac{3\sqrt{2}}{\pi}v} \tag{53}$$

Step 7: Calculate angle for converter terminals by Eq. (54):

$$\alpha, \gamma = \arccos\left(\frac{v_d + \frac{\sqrt{3}}{\pi}x_c i_d}{v_{do}}\right) \tag{54}$$

Step 8: Calculate the active power transmission line losses by Eq. (55):

$$p_{loss} = \sum_{i=1}^{N_g} p_{gi} - \sum_{j=1}^{N} p_{loadj} \tag{55}$$

where p_{loss} represents per unit power loss of the power system and p_{loadj} is the active load of bus j.

Step 9: Calculate F_i by Eq. (49).

A block diagram for the calculation of fitness values by the proposed algorithm is given in Figure 5.

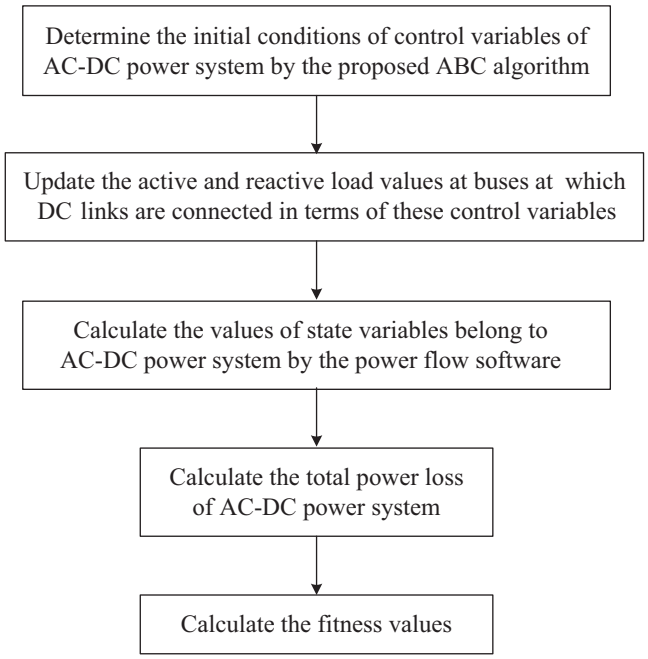

Figure 5. Block diagram for calculation of fitness values.

6. Simulation results

The proposed method is examined on three test systems: the modified IEEE 14-bus test system [37], the modified IEEE 30-bus test system [38], and the modified 39-bus New England test system [39,40].

The stopping criterion is selected as 100 iterations. The problem is solved by different bee sizes and the proposed algorithm is run 25 times for these sizes. The software used for the proposed method is real-coded and run on a computer with I3 CPU 2.4 GHz, 2 GB RAM.

Simulations are performed for 2 cases: continuous and discrete. Under the continuous case all variables in the power system are considered as continuous. Under the discrete case the transformer tap ratios and shunt reactive compensators are considered as discrete and the other variables are considered as continuous. The transformer and the capacity step are considered to be 0.01 p.u. Furthermore, the ideal operating case is satisfied by considering $q_d = |0.5 * p_d|$ [41].

6.1. The modified IEEE 14-bus test system

The modified IEEE 14-bus test system consists of the establishment of a two-terminal DC link between buses 4 and 5 of the original IEEE 14-bus test system [37]. Buses 4 and 5 are the rectifier and inverter terminals of the DC link, respectively. The system consists of two generators, three transformers, twenty AC lines, two switchable VAR compensators, and three synchronous condensers. The simulation is performed for two cases with light and heavy loads mentioned in [37]. As a result of the performed experiments the best population size is determined to be 20. Half of the population is selected as worker bees and the other half as nonworker bees.

The variations in the power losses versus the iteration number for both load cases are shown in Figure 6 for both discrete and continuous cases.

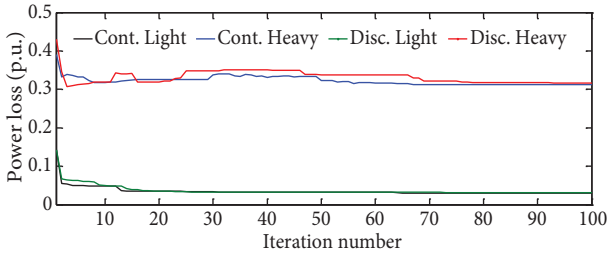

Figure 6. Variations in the power losses versus the iteration number for both load cases and for both discrete and continuous cases.

The comparative results for the fitness values of this system are given in Table 1. As seen from Table 1, the results of the ABC algorithm for both discrete and continuous cases are better than those obtained by the linear programming technique [37] and GA [40].

As seen from Table 1, the power losses obtained by the ABC algorithm for the discrete case are less than those obtained by the linear programming technique [37] and GA [40] by 27.47% and 13.11%, respectively. The power losses obtained by the proposed algorithm for the continuous case are also less than those obtained by the linear programming technique [37] and GA [40] by 29.88% and 16.00%, respectively. The power losses obtained by the ABC algorithm for both discrete and continuous cases are less than those obtained by the linear programming technique [37] by 6.14% and 7.17%, respectively. The computational times for both load cases are almost the same (39.48 s).

Table 1. Comparative results for light and heavy load conditions of the modified IEEE 14-bus test system.

		Fitness value			
	Algorithm	Minimum	Maximum	Average	Time (s)
Light load	ABC algorithm (Discrete)	0.030824	0.039952	0.035388	39.48
	ABC algorithm (Continuous)	0.029799	0.038003	0.033901	
	Linear programming technique [37]	0.0425	–	–	–
	GA [40]	0.035476	0.041244	0.03836	67.65
Heavy load	ABC algorithm (Discrete)	0.316028	0.334024	0.325026	
	ABC algorithm (Continuous)	0.312533	0.332707	0.322620	
	Linear programming technique [37]	0.3367	–	–	
	GA [40]	–	–	–	

6.2. The modified IEEE 30-bus test system

The system data of this system is given in [38]. The study is performed for two different cases [38].

First Case: the modified IEEE 30-bus test system consists of the establishment of a two-terminal DC link between buses 2 and 14 of the original IEEE 30-bus test system.

Second Case: the modified IEEE 30-bus test system consists of the establishment of a two-terminal DC link between buses 2 and 16 of the original IEEE 30-bus test system.

As a result of the performed experiments the best population size is determined to be 20. The comparative results for the fitness values of this system are given in Table 2. As seen from Table 2, the results of the ABC algorithm for both discrete and continuous cases are better than those obtained by the linear programming technique [38] and GA [40] for both discrete and continuous cases. For both HVDC cases the computational time obtained by the ABC algorithm for both discrete and continuous cases is almost the same (57.79 s).

Table 2. Comparative results for both HVDC cases of the modified IEEE 30-bus test system.

		Fitness value			
	Algorithm	Minimum	Maximum	Average	Time (s)
First case	ABC algorithm (Discrete)	0.123874	0.140204	0.132039	57.79
	ABC algorithm (Continuous)	0.116782	0.139526	0.128154	
	Linear programming technique [38]	0.2841	–	–	–
	GA [40]	0.124065	0.142020	0.1330425	74.86
Second case	ABC algorithm (Discrete)	0.119300	0.135684	0.127492	
	ABC algorithm (Continuous)	0.114766	0.135622	0.125194	
	Linear programming technique [38]	0.2811	–	–	
	GA [40]	0.120150	0.135989	0.1280695	

The variations in the power losses versus the iteration number for both HVDC cases are shown in Figure 7 for both discrete and continuous cases.

As seen from Table 2, for HVDC Case A, the power losses obtained by the ABC algorithm for the discrete case are less than those obtained by the linear programming technique [38] and GA [40] by 56.40% and 0.10%, respectively. The power losses obtained by the proposed algorithm for the continuous case are also less than those obtained by the linear programming technique [38] and GA [40] by 58.89% and 5.82%, respectively. For HVDC Case B, the power losses obtained by the ABC algorithm for the discrete case are less than those obtained by the linear programming technique [38] and GA [40] by 57.56% and 0.66%, respectively. The power losses obtained by the proposed algorithm for the continuous case are also less than those obtained by the linear programming technique [38] and GA [40] by 59.17% and 4.44%, respectively.

6.3. The modified New England 39-bus test system

The modified New England 39-bus test system consists of the establishment of a two-terminal DC link between buses 4 and 14 of the original New England 39-bus test system [39,40]. The lower and upper limits of the transformer tap ratio are 0.9 p.u. and 1.1 p.u., respectively. As a result of the performed experiments the best population size is determined to be 40 and the computational time is calculated as 86.24 s.

A variation in the power loss versus the iteration number for both discrete and continuous cases is shown in Figure 8.

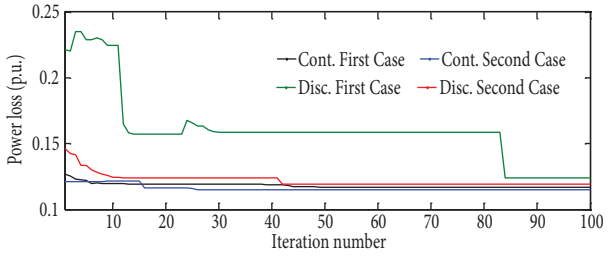

Figure 7. Variations in the power losses versus the iteration number for both HVDC cases and for both discrete and continuous cases.

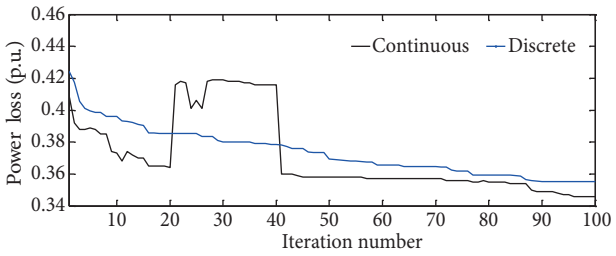

Figure 8. Variations in the power losses versus the iteration number for both discrete and continuous cases.

The comparative results for the fitness values of this system are given in Table 3. As seen from Table 3, the results of the ABC algorithm for both discrete and continuous cases are better than those obtained by GA [40].

As seen from Table 3, the power losses obtained by the ABC algorithm for both discrete and continuous cases are less than those obtained by GA [40] by 4.43% and 7.01%, respectively.

Table 3. Fitness values obtained by the ABC algorithm and GA [40] for the modified New England 39-bus test system.

	Fitness value			
Algorithm	Minimum	Maximum	Average	Time (s)
ABC algorithm (Discrete)	0.355340	0.397128	0.376234	86.24
ABC algorithm (Continuous)	0.345743	0.388321	0.371320	
GA [40]	0.371844	0.564434	0.468139	121.4

7. Conclusion and discussion

In the current study the ABC algorithm is applied to the ORPF problem of AC-DC power systems for the first time. The algorithm is tested on three test systems. As seen from Tables 1–3, the results of the ABC algorithm are better than those of linear programming [37,38] and GA [40] for all test systems. Although the active power transferred by the DC link obtained by this approach is close to that obtained by the linear programming technique [37], the power loss is less than that obtained by the linear programming technique [37]. The computational times of the proposed algorithm are also shorter than those of other approaches. This study shows that the ABC algorithm can be applied to the ORPF problem of large-scale multiterminal AC-DC systems. The population size of the algorithm is determined independently from the size of the system and so it is necessary to perform trials for each system in terms of the population size.

Nomenclature

λ_{ij}	A random number between –1 and 1
P_{gk}, Q_{gk}	Output active and reactive powers of the generator connected to k^{th} bus
P_{lk}, Q_{lk}	Active and reactive loads of k^{th} bus
P_k, Q_k	Active and reactive powers given to ac transmission line at k^{th} bus
P_{dk}	Active power given to dc transmission link at k^{th} bus
Q_{dk}	Reactive power absorbed by converter at k^{th} bus
Q_{sk}	Reactive power of the shunt compensator at k^{th} bus
I_r, I_i	AC currents at rectifier and inverter terminals
δ	Bus voltage angles
V	Bus voltage magnitudes
N	Number of all buses of the power system
k	Peak number on the load per period
P_{dr}, P_{di}	Active powers at rectifier and inverter terminals
δ_{kj}	Angular difference between buses k and j
R_{cr}, R_{ci}	Commutating resistances of rectifier and inverter
X_{cr}, X_{ci}	Commutating reactances of rectifier and inverter
Y_{bus}	Bus admittance matrix
G_{kj}, B_{kj}	Transfer conductance and susceptance between buses k and j of the bus admittance matrix
x, u	State and control variables of AC-DC system
R_{dc}	DC link resistance
I_d	DC current
V_{dr}, V_{di}	DC voltages at rectifier and inverter terminals
t	Effective transformer tap ratio
α	Excitation angle for rectifier
γ	Extinction angle for inverter
w_{ij}	Nourishment source position
V_{dor}, V_{doi}	Unload DC voltages at rectifier and inverter terminals
$w_{\max,j}, w_{\min,j}$	Upper and lower limits of the nourishment source position
fit_i	Nectar amount of the i^{th} nourishment source
N_g	Number of generator buses
N_l	Number of load buses
D	Number of optimization parameters
N_s	Number of shunt compensators
n	Bridge number in series
N_T	Number of transformers
φ_r, φ_i	Phase angle between the AC voltage and the fundamental component of AC current at rectifier and inverter terminals
Q_{dr}, Q_{di}	Reactive powers absorbed by the converters at rectifier and inverter terminals
SN	Number of the nourishment sources
p_{gslack}	Slack bus active power output
$rand\,(0,1)$	A random number between 0 and 1
P_{acbase}	AC base active power
V_{acbase}	AC base voltage
I_{acbase}	AC base current
Z_{acbase}	AC base impedance
sp_i	Designation probability of i^{th} nourishment source
F_i	i^{th} fitness value
p_{gi}	Per unit active power of i^{th} generator
q_{gi}	Per unit reactive power of i^{th} generator
v_{li}	Per unit voltage of i^{th} load bus
v_{gi}	Per unit voltage of i^{th} generator
K	Penalty weight
p_{load}	Active load
q_{load}	Reactive load
p_{loss}	Per unit power loss of power system

References

[1] Wu YC, Debs AS, Marsten RE. A nonlinear programming approach based on an interior point method for optimal power flows. International Power Conference Athens Power Tech, Vol. 1, 5–8 Sep 1993, pp. 196–200.

[2] Grudinin N. Reactive power optimization using successive quadratic programming method. IEEE T Power Syst 1998; 13: 1219–1225.

[3] Mangoli MK, Lee KY, Park YM. Optimal real and reactive power control using linear programming. Electr Pow Syst Res 1993; 26: 1–10.

[4] Gomes JR, Saavedra OR. Optimal reactive power dispatch using evolutionary computation: extended algorithms. IEEE Proceedings Generation, Transmission and Distribution 1991; 146: 586–592.

[5] Iba K. Reactive power optimization by genetic algorithm. IEEE T Power Syst 1994; 9: 685–692.

[6] Wu QH, Cao YJ, Wen JY. Optimal reactive power dispatch using an adaptive genetic algorithm. Int J Elec Power 1998; 20: 563–569.

[7] Liu Y, Ma L, Zhang J. Reactive power optimization by GA/SA/TS combined algorithms. Int J Elec Power 2002; 24: 765–769.

[8] Ayan K, Kılıç U. Optimal Reactive Power Flow Solution with Chaotic Artificial Bee Colony. 6th International Advanced Technologies Symposium (IATS'11), Electrical & Electronics Technologies, May 2011, Elazığ, Turkey.

[9] Çobanlı S, Öztürk A, Güvenç U, Tosun S. Active power loss minimization in electric power systems through artificial bee colony algorithm. Int Rev Electr Eng-I 2010; 5: 2217–2223.

[10] Yan W, Lu S, Yu DC. A novel optimal reactive power dispatch method based on an improved hybrid evolutionary programming technique. IEEE T Power Syst 2004; 19: 913–918.

[11] Yoshida H, Kawata K, Fukuyama Y, Takayama S, Nakanishi Y. A particle swarm optimization for reactive power and voltage control considering voltage security assessment. IEEE T Power Syst 2000; 15: 1232–1239.

[12] Xiong H, Cheng H, Li H. Optimal reactive power flow incorporating static voltage stability based on multi-objective adaptive immune algorithm. Energ Convers Manage 2008; 49: 1175–1181.

[13] Varadarajan M, Swarup KS. Differential evolutionary algorithm for optimal reactive power dispatch. Int J Elec Power 2008; 30: 435–411.

[14] Latorre HF, Ghandhari M. Improvement of power system stability by using a VSC–HVDC. Int J Elec Power 2011; 33: 332–339.

[15] Sato H, Arrillaga J. Improved load-flow techniques for integrated AC-DC systems. P I Electr Eng 1969; 116: 525–532.

[16] Messalti S, Belkhiat S, Saadate S, Flieller D. A new approach for load flow analysis of integrated AC–DC power systems using sequential modified Gauss–Seidel methods. International Transactions on Electrical Energy Systems 2012; 22: 421–432.

[17] Kılıç U, Ayan K. Optimal power flow solution of two-terminal HVDC systems using genetic algorithm. Electr Eng 2013; 96: 65–77.

[18] Yalçın F, Arifoğlu U. Optimal reactive power flow solution in multi-terminal ac-dc systems based on artificial bee colony algorithm. Turk J Elec Eng & Com Sci 2014; 22: 1159–1176.

[19] Fudeh H, Ong CM. A simple and efficient AC-DC load-flow method for multi-terminal DC systems. IEEE T Power Ap Syst 1981; 100: 4389–4396.

[20] Kimbark E. Direct Current Transmission. New York, NY, USA: Wiley-Interscience, 1971, pp. 9.

[21] Reeve J, Fahny G, Stott B. Versatile load flow method for multi-terminal HVDC systems. IEEE T Power Ap Syst 1977; 96: 925–933.

[22] Arifoğlu U. Load flow based on Newton's method using Norton equivalent circuit for an AC-DC multi-terminal system. Eur T Electr Power 1999; 9: 167–174.

[23] Baradar M, Ghandhari M, Van Hertem D, Kargarian A. Power flow calculation of hybrid AC/DC power systems. IEEE Power and Energy Society General Meeting, 2–26 July 2012, pp. 1–6.

[24] Karaboga D. An idea based on honey bee swarm for numerical optimization. TECHNICAL REPORT-TR06. Erciyes University, Engineering Faculty, Computer Engineering Department, 2005.

[25] Kwannetr U, Leeton U, Kulworawanichpong T. Optimal power flow using artificial bees algorithm. International Conference on Advances Energy Engineering, Beijing, China, 19–20 June 2010, pp. 215–218.

[26] Srinivasa Rao R, Narasimham SVL, Ramalingaraju M. Optimization of distribution network configuration for loss reduction using artificial bee colony algorithm. International Journal of Electrical Power and Energy Systems Engineering 2008; 1: 708–714.

[27] Kılıç U, Ayan K. Optimizing power flow of AC-DC power systems using artificial bee colony algorithm. Int J Elec Power 2013; 53: 592–602.

[28] Hemamalini S, Simon SP. Artificial bee colony algorithm for economic load dispatch problem with non-smooth cost functions. Electr Pow Compo Sys 2010; 38: 786–803.

[29] Hemamalini S, Simon SP. Dynamic economic dispatch using artificial bee colony algorithm for units with valve-point effect. International Transactions on Electrical Energy Systems 2011; 21: 70-81.

[30] Lu CN, Chen SS, Ong CM. The incorporation of HVDC equations in optimal power flow methods using sequential quadratic programming techniques. IEEE T Power Syst 1988; 3: 1005–1011.

[31] Mustafa MW, Abdul Kadir AF. A modified approach for load flow analysis of integrated AC-DC power systems. Proceedings TENCON 2000, Kuala Lumpur, Malaysia, 2000 Vol. 2, pp. 108–113.

[32] Kundur P. Power System Stability and Control. New York, NY, USA: McGraw-Hill, 1994, pp. 501.

[33] Ayan K, Kılıç U. Artificial bee colony algorithm solution for optimal reactive power flow. Appl Soft Comput 2012; 12: 1477–1482.

[34] Karaboga D, Akay B. A comparative study of artificial bee colony algorithm. Appl Math Comput 2009; 214: 108–132.

[35] Sonmez M. Artificial bee colony algorithm for optimization of truss structures. Appl Soft Comput 2011; 11: 2406–2418.

[36] He Y, Jian C. Clonal selection algorithm with adaptive mutation and roulette wheel selection. Computational intelligence and security workshops, Harbin, China, 15–17 December 2007, pp. 93–96.

[37] Sreejaya P, Iyer SR. Optimal reactive power flow control for voltage profile improvement in AC-DC power systems. Power Electronics, Drives and Energy Systems Power India, New Delhi, India, 20–23 December 2010, pp. 1–6.

[38] Taghavi R, Seifi A. Optimal reactive power control in hybrid power systems. Electr Pow Compo Sys 2012; 40: 741–758.

[39] Kılıç U, Ayan K. Transient stability constrained optimal power flow solution of AC–DC systems using genetic algorithm. The 3rd International Conference on Electric Power and Energy Conversion Systems, 2–4 Oct 2013 Yıldız Technical University, İstanbul, Turkey, pp. 1-6.

[40] Kılıç U, Ayan K, Arifoğlu U. Optimizing reactive power flow of HVDC systems using genetic algorithm. Int J Elec Power 2014; 55: 1–12.

[41] Arrillaga J, Liu YH, Watson NR. Flexible Power Transmission: The HVDC Options. Chichester, UK: John Wiley & Sons, 2007, pp. 10.